Journal of The Electrochemical Society, **154** (3) D182-D187 (2007)
0013-4651/2007/154(3)/D182/6/$20.00 © The Electrochemical Society

Optimization of a Pretreatment for Copper Electroless Deposition on Ta Substrates

Chang Hwa Lee,[a,*] Seung Hwan Cha,[b] Ae Rim Kim,[a] Ji-Ho Hong,[c] and Jae Jeong Kim[a,,z]**

[a]*Research Center for Energy Conversion and Storage, School of Chemical and Biological Engineering, College of Engineering, Seoul National University, Kwanak-gu, Seoul 151-742, Korea*
[b]*LG Philips LCD Research and Development Center, Anyang-shi, Gyongki-do 431-080, Korea*
[c]*Dongbu Electronics, Department of Advanced Nano-tech Development, Umsung-kun, Chungbuk 369-852, Korea*

We investigated pretreatment methods for Cu electroless deposition on a Ta substrate. The native oxide on the substrate was effectively etched by the addition of HNO_3 to a HF diluted solution and this was confirmed though X-ray photoelectron spectroscopy and chronopotentiometry. To form the Pd catalyst for Cu electroless deposition, a two-step Sn sensitization and Pd activation was carried out. The oxide removal enhanced the adsorption of the Sn ions on the Ta substrate and led to well distributed Pd clusters through Pd activation. By measuring the resistivity of the film, the Sn sensitization time and the Pd activation time were optimized through changes in the incubation time, at which the sheet resistance abruptly decreased by the film formation via the coalescence of Cu grains. The resistivity of the Cu electroless film deposited using the optimized pretreatment conditions was 3.59 $\mu\Omega$ cm, which was further reduced to 2.7 $\mu\Omega$ cm through an annealing process.
© 2007 The Electrochemical Society. [DOI: 10.1149/1.2432074] All rights reserved.

Manuscript submitted February 8, 2006; revised manuscript received November 6, 2006.
Available electronically February 1, 2007.

Recently, electroless deposition has been applied to the areas of microelectromechanical systems (MEMS),[1,2] thin-film deposition for bio applications,[3,4] and fuel cells,[5,6] as well as ultralarge scale integrated circuits (ULSIs)[7,8] or printed circuit boards (PCBs),[9] due to its low cost, low temperature process, and simplified procedures compared to those of physical vapor deposition (PVD) and chemical vapor deposition (CVD). Because the electroless deposition occurs through the oxidation reaction of a reducing agent, it is possible to deposit metals on metallic, ceramic,[10] glass,[11] and polymeric substrates[12] without supplying an external electron source. However, to deposit metal films heterogeneously on these substrates, appropriate surface treatments and catalyzing methods are required, depending on the type of substrate in question.

In particular, for the application of Cu electroless deposition to ULSIs, generally, Pd catalyst formation should be preceded on the barrier layers such as Ta, TaN, and TiN through a one-step Pd displacement, one-step Sn-Pd activation, or two-step Sn sensitization-Pd activation.[13-16]

In previous research on TiN substrates, the pretreatment process was optimized including Ti oxide etching and Pd activation by the displacement method prior to electroless Cu deposition. The optimization was achieved by monitoring the sheet resistance to identify the incubation time, which is defined as the time at which the Cu film that is being formed becomes continuous. At that time, the sheet resistance decreases dramatically.[13] However, the TiN layer has some drawbacks as a barrier for Cu metallization because the columnar structure of the TiN deposited by PVD or CVD provides a mechanism for the fast diffusion of Cu to the underlying substrate.[17] On the other hand, it is known that Ta is thermodynamically stable with respect to Cu and a Ta-based barrier layer has a significantly higher resistance to Cu diffusion.[18,19]

Although Cu electroless deposition on Ta-based barrier layers has been performed, the pretreatment process was not fully established regarding Ta oxide removal and Pd activation. Thus, in this study we present a pretreatment procedure for the Ta barrier layer for Cu electroless deposition, optimizing the removal of Ta oxide from the surface and Pd catalyst formation.

* Electrochemical Society Student Member.
** Electrochemical Society Active Member.
z E-mail: jjkimm@snu.ac.kr

Experimental

The substrates used in this experiment were composed of a Ta (7.5 nm)/TaN(7.5 nm)/Si wafer. To remove the native oxide on the Ta surface, either a 1 vol % HF solution or a mixture of 1 vol % HF and 1.4 vol % HNO_3 was used. The etching time was optimized by monitoring the variations of the sheet resistance as a function of etching time. Chronopotentiometry was carried out in the electrolyte which contained 0.1 M HCl using an Ag/AgCl electrode and Pt wire as a reference and a counter electrode, respectively, to confirm the existence of the oxide on the surface electrochemically. After Ta oxide etching, two Pd activation methods were applied to form the catalyst for Cu nucleation. The first was a one-step Pd activation performed by a displacement reaction in the solution containing 5×10^{-4} M $PdCl_2$, 0.04 M HCl, and 0.14 M HF, which was previously optimized for TiN substrates.[13] The other, known as the two-step Sn sensitization-Pd activation method, was carried out by sequentially dipping the substrate in solutions composed of 0.01 M $SnCl_2 \cdot 2H_2O$ and 0.1 M HCl for 2 min and 5×10^{-4} M $PdCl_2$ and 0.04 M HCl for 20 s, respectively. The optimum dipping time was determined by measuring the incubation time, at which point the sheet resistance decreases dramatically as the Cu film that is being formed becomes continuous. Following the Sn sensitization step in a range of individual times (1, 2, 3, and 5 min), Pd activation was carried out on each Sn-treated samples for 20 s. Then, monitoring the abrupt decrease in sheet resistance (during Cu electroless deposition) for each sample, the optimal Sn sensitization was experimentally determined. Likewise, following the Sn sensitization for 3 min, Pd activation was performed for 5, 10, 20, and 50 s, respectively. Then, Pd activation time was optimized from the incubation time measured during Cu electroless deposition. The base electrolyte consisted of 0.025 M $CuSO_4 \cdot 5H_2O$, 2.9 g/L paraformaldehyde ($(HCHO)_n$), 0.054 M ethylenediaminetetraacetic acid (EDTA) and 0.49 M KOH. To reduce the incorporation of oxygen into the film, 0.1 g/L 2,2′-dipyridyl, which is a well-known stabilizer, was added in the base electrolyte and the deposition temperature was maintained at 70°C.

The sheet resistance change of the Ta substrate with respect to etching time was measured by a four-point probe. The surface analyses were carried out using X-ray photoelectron spectroscopy (XPS) and atomic force microscopy (AFM). A potentiostat/galvanostat (Versastat II, EG&G Princeton Applied Research) was used for chronopotentiometry and transmission electron microscopy (TEM) was used to examine the Pd catalysts on the Ta substrate. An optical

Downloaded 04 Jul 2010 to 147.46.246.152. Redistribution subject to ECS license or copyright; see http://www.ecsdl.org/terms_use.jsp

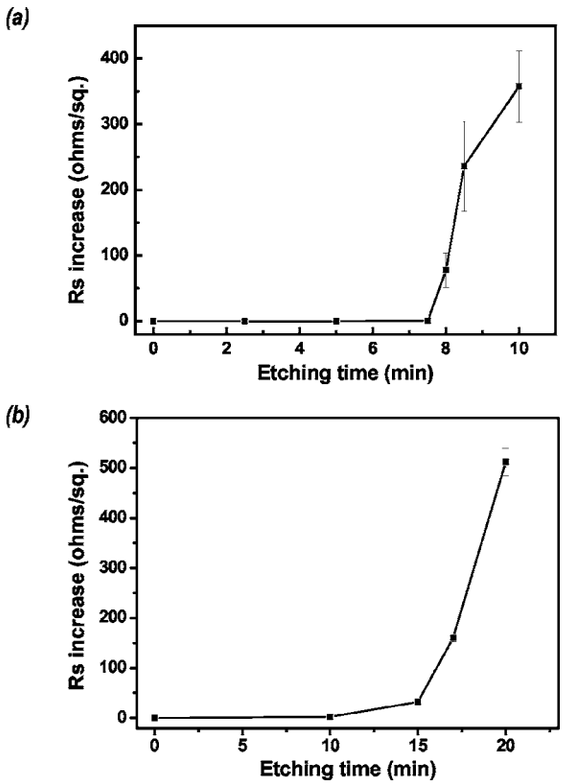

Figure 1. Evolution of sheet resistance with time in two different Ta cleaning solutions: (a) 1 vol % diluted HF and (b) 1 vol % diluted HF with the addition of 1.4 vol % HNO_3.

microscope was used for measuring the contact angles and comparing the wetting properties. Field-emission scanning electron microscopy (FE-SEM) and Auger electron spectroscopy (AES) were employed to check the thickness and depth profile of the Cu.

Results and Discussion

In general, the removal of oxide is essential to form Pd catalysts on low conductive barrier layers. Because the oxide passivation layer interrupts the displacement reaction between Pd ions and the barrier layer, which makes Cu electroless deposition impossible to occur. The chemical etching of the native oxide on the surface enhances the hydrophilicity related to the adhesion of Pd catalysts.[13,20]

Figure 1 shows the change in the sheet resistance with time before and after Ta oxide etching in the two different etching solutions. As shown in Fig. 1a, an abrupt increase in the sheet resistance difference appeared after about 7.5 min of etching in a 1 vol % HF solution. On the other hand, this was delayed by 15 min when etched in a solution with 1.4 vol % HNO_3 and 1 vol % HF. This abrupt increase in the sheet resistance difference is considered to be due to the etching of the Ta layer after the oxide removal or to an increase in the surface roughness. This was clarified through XPS and AFM analyses afterward.

To confirm the removal of the Ta oxide, XPS was carried out on the substrate after Ta oxide etching for the optimized time based on changes in the sheet resistance with time for the two different solutions. Figure 2b shows the Ta 4f peaks after the oxide etching in the 1 vol % HF solution for 7.5 min. Compared with the initial Ta surface (Fig. 2a), Ta_2O_5 still remains on the surface, as it was originally. On the other hand, the peak of the Ta 4f peak corresponding to Ta_2O_5 had decreased, compared to that of the initial Ta, when the Ta oxide was etched in the solution containing 1.4 vol % HNO_3 and 1 vol % HF, as shown in Fig. 2c. Although the relative decrease in Ta oxide peaks through etching with the HNO_3-added HF solution

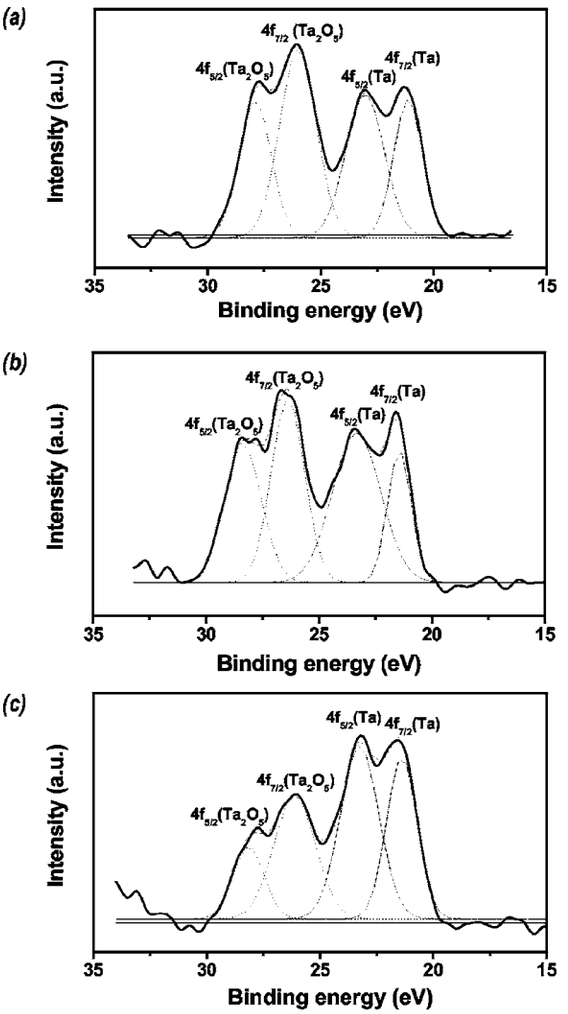

Figure 2. Ta 4f XPS spectra of (a) initial Ta substrate, (b) Ta substrate etched by a 1 vol % HF solution, and (c) Ta substrate etched by a mixture of 1 vol % HF and 1.4 vol % HNO_3.

was observed through XPS, oxide peaks still existed. This is considered that the Ta surface was partially reoxidized during sample transferring. Indeed, this was confirmed that the reoxidation occurred within a few minutes of exposure to air, in the result of additional XPS analyses.

To exclude the influence by reoxidation, the coulometric reduction method (CRM)[21,22] was adopted. When the current is applied to the Ta surface covered with Ta oxide, Ta oxide begins to reduce through the following reaction: $Ta_2O_5 + 10H^+ + 10e^- \rightarrow 2Ta + 5H_2O$ and a sharp potential drop appears. On the basis of this, applying a constant current of 50 μA to 1 cm^2 of the oxide-etched Ta substrates by the respective etching solutions, the electrode potentials vs an Ag/AgCl reference electrode were measured as a function of time. As shown in Fig. 3a and b, chronopotentiograms of Ta pretreated with 1 vol % HF solution displayed a transition time of 30 s in both 7.5 min and 10 min, which means Ta oxides still exist even after Ta oxide etching. On the other hand, in the sample etched Ta oxide with HNO_3-added HF solution, no transition region was observed, as shown in Fig. 3c, which proves that the oxide was completely removed by HNO_3-containing HF solution.

The surface morphologies of the substrates that were treated with the different etching methods were compared to the initial Ta substrate, as shown in Fig. 4a-c. When the Ta oxide was etched in the 1 vol % HF solution for 7.5 min, the surface roughness increased

Downloaded 04 Jul 2010 to 147.46.246.152. Redistribution subject to ECS license or copyright; see http://www.ecsdl.org/terms_use.jsp

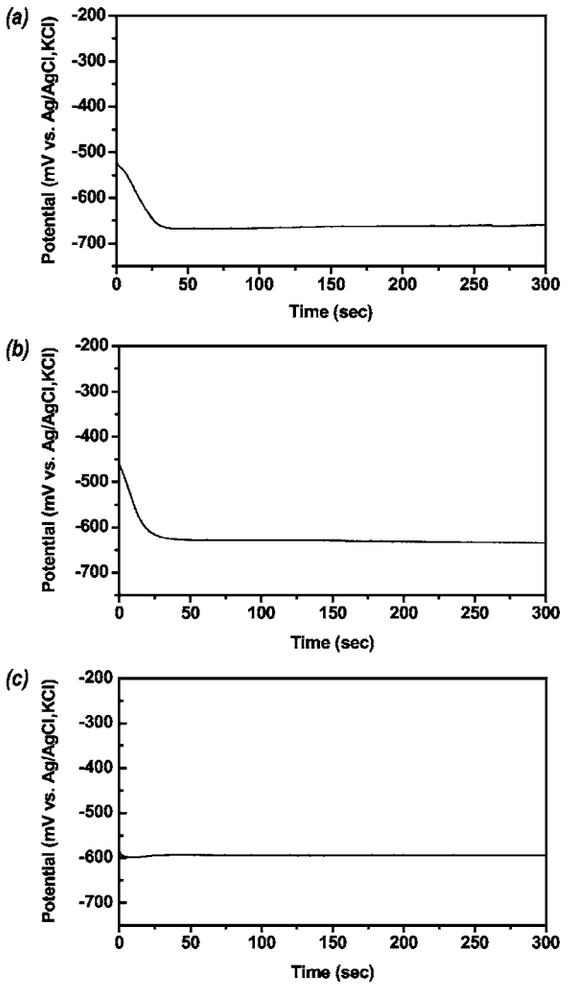

Figure 3. Chronopotentiogram at 50 μA of Ta substrates etched for (a) 7.5 min and (b) 10 min in a 1 vol % HF solution, and (c) 15 min in a mixture of 1 vol % HF and 1.4 vol % HNO_3 solution.

rapidly up to 1.1 nm, which corresponded to a 15% increase against the Ta thickness, while it slightly increased from the 0.13 nm of the initial Ta substrate to 0.2 nm in the mixture of 1 vol % HF and 1.4 vol % HNO_3. Additionally, the pitting corrosion was observed on the Ta surface etched with 1 vol % HF solution due to a partial etching of the oxide layer (Fig. 4d). Thus, it was considered that the increase in the sheet resistance after 7.5 min of etching in the 1 vol % HF solution determined by AFM and FE-SEM measurements was attributed not only to Ta oxide etching but also to an increase in the surface roughness by pitting corrosion.

Although many researchers have added HNO_3 to a diluted HF solution to remove the Ta oxide on the surface, the effect of HNO_3 is not clear. In the case of silicon (Si), mixtures of HF and HNO_3 are well-known solutions for etching Si/Si oxides through oxidization of the silicon by HNO_3 followed by the etching of the oxide by HF nearly simultaneously. The $HNO_3/H_2O/HF$ treated Ta sample had a very smooth surface after the oxide etching at low concentrations of HNO_3 and HF, while a significant increase in the roughness was visible at higher concentrations of HNO_3 and HF.[23] In addition, in the Pourbaix diagram of Ta in 1.0 M HF, which shows the thermodynamic stability of the species as a function of the potential and pH, TaF_7^{2-} becomes more stable than Ta_2O_5 as the pH decreases.[24] Therefore, the addition of HNO_3 enables a more effective removal of the Ta oxides due to the decreased pH and also lowers surface roughness by acting as an oxidizing agent, controlling the removal rate of the Ta oxides.

The pretreated Ta substrate should be activated with catalysts such as palladium (Pd) to allow Cu reduction to occur heterogeneously on the surface. Although one-step Pd activation, where Pd ions are reduced by electrons generated from the oxidation of the substrate, was attempted for 20 s, as in the case of TiN substrates,[13] it was confirmed through microscopy and XPS that Pd particles were not formed on the surface. Even though the oxide was removed, the Ta substrate was considered to be oxidized to the Ta oxide, not TaF_7^{2-}, because Ta_2O_5 is thermodynamically stable in the Pd activation solution with a mixed potential of 0.214 V (vs. SCE) and pH of 0.51 (measured at 18°C). The passivation of the Ta substrate makes the formation of the Pd catalysts difficult by preventing the supply of electrons to the Pd ions.

Alternatively, a two-step Sn sensitization and Pd activation method was used to form the catalytic nuclei on the Ta substrate. In this method, the electrons generated by the oxidation of Sn^{2+} to Sn^{4+}

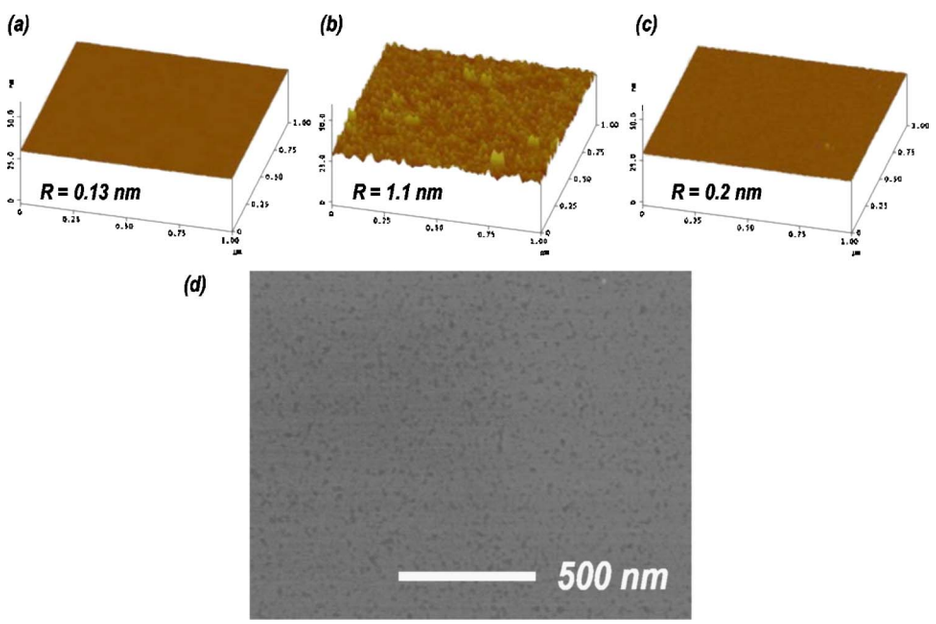

Figure 4. (Color online) AFM images of (a) initial Ta substrate, (b) the Ta substrate etched by a 1 vol % HF solution, and (c) the Ta substrate etched by a mixture of 1 vol % HF and 1.4 vol % HNO_3 and (d) SEM surface image of (b).

Downloaded 04 Jul 2010 to 147.46.246.152. Redistribution subject to ECS license or copyright; see http://www.ecsdl.org/terms_use.jsp

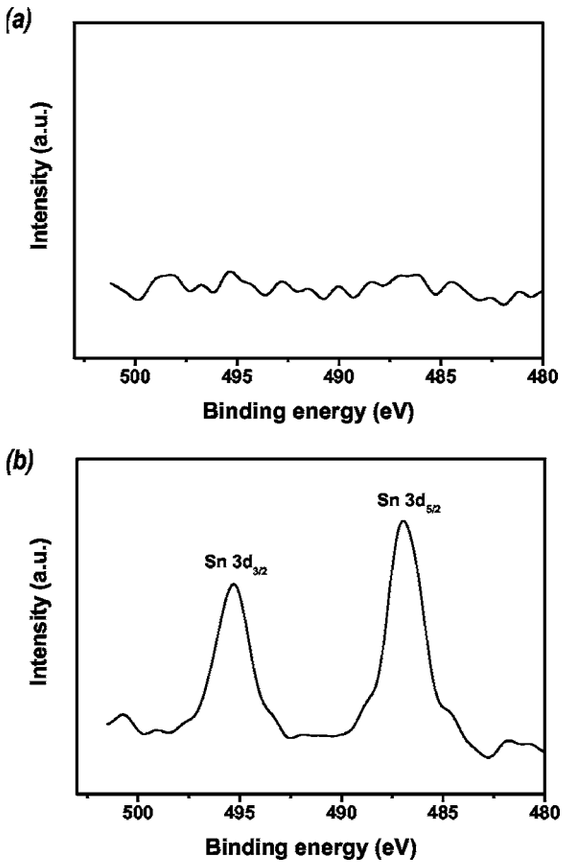

Figure 5. XPS spectra of the Sn 3d peak on Ta samples sensitized (a) without oxide etching and (b) after oxide etching with a mixture of 1 vol % HF and 1.4 vol % HNO_3.

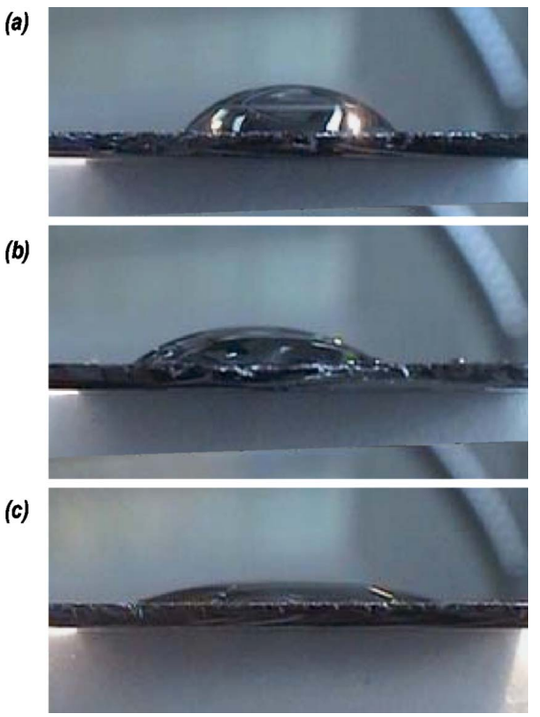

Figure 6. (Color online) Optical images for measuring contact angles of Ta substrates (a) without oxide etching, (b) etched with a 1 vol % HF, and (c) etched with a mixture of 1 vol % HF and 1.4 vol % HNO_3.

adsorbed on the substrate surface reduced the Pd^{2+} ions to metallic Pd. Because it does not accompany the oxidation of the substrate, nonconductive materials such as polymers, glasses, and ceramics can be activated with the catalysts, even though a surface treatment prior to Sn sensitization is sometimes necessary to ensure sufficient adhesion of Pd nuclei.[25] As shown in Fig. 5a, Sn was not detected on the Ta surface in the absence of Ta oxide etching process, while the Sn $3d_{5/2}$ peak corresponding to Sn^{2+} (486.9 eV) was observed on the pretreated Ta in the mixture of HF and HNO_3 solutions (Fig. 5b).

To verify the effect of the diluted HF-HNO_3 solution on the hydrophilicity, contact angle measurements were carried out. Figure 6 shows optical microscope images of the water droplet of 35 μL dropping on the different types of Ta surfaces. While, the contact angles calculated from the images were 21.8° (Fig. 6a) and 16.4° (Fig. 6b) on the initial Ta and Ta substrate pretreated with 1 vol % HF solution, respectively, and that of Ta substrate etched with HF-HNO_3 solutions was 8.0° (Fig. 6c), which represents the addition of HNO_3 enhanced the hydrophilicity of the Ta surface and aided the Sn ions in effectively adsorbing onto the Ta substrates.

Pd activation was performed on the Ta substrates treated with Ta oxide etching and subsequent Sn sensitization. Figure 7a presents TEM images of the Pd particles with a height of 7.8 ± 1.1 nm and a diameter of 10.9 ± 2.1 nm that were formed by Pd activation. Pd was confirmed by the XPS analysis, as shown in Fig. 7b.

To optimize the Sn sensitization time and the Pd activation time, the incubation time for Cu electroless deposition, which is defined as the time at which the sheet resistance dropped abruptly, was measured as exhibited in Fig. 8. After Sn sensitization for various times at a fixed Sn concentration and subsequent Pd activation for 20 s, the incubation time was measured during Cu electroless deposition as shown in Fig. 8a. The incubation time eventually became saturated after about 3 min of Sn sensitization. This implies time is required for the Sn ions to adsorb and provide a site for Pd reduction on the surface, even though it may depend on the concentration of the Sn source. In the case of Pd activation, the incubation time was measured as differing from the activation time after evenly treating with 3 min of Sn sensitization, as shown in Fig. 8b. The incubation time was virtually the same regardless of the Pd activation time, which shows that the displacement reaction of Pd occurred rapidly compared to the adsorption of Sn.

Considering the incubation time and the resistivity of the Cu film, a Sn sensitization time of 3 min and a Pd activation time of 20 s were selected to provide optimum pretreatment conditions. Figure 9a shows the cross-sectional image of the Cu film deposited after 100 s at a temperature of 70°C using the optimized pretreatment conditions and the AES depth profiling of the as-deposited Cu film was done as shown in Fig. 9b. Although the resistivity of Cu film was 3.59 μΩ cm at 110 nm thick, which was higher than the bulk resistivity of Cu (1.7 μΩ cm), the incorporation of oxygen inside the film, which is a main factor causing increases in the resistivity, was not observed due to the use of the surfactant. Besides the resistivity could be reduced to (2.7 μΩ cm) through thermal annealing at 400°C by increasing the grain sizes.

The poor adhesion of Cu electroless film was a problem after the deposition, however it was significantly improved though the thermal annealing and passed the 3M tape test. Also the adhesion of as-deposited film of which thickness was reduced down to 50 nm by a dilution of the electrolyte could be enhanced even without the addition of surfactants.[26] This indicates that an increase in tensile stress by an increase in the thickness is one of the main factors in degrading the adhesion property even at the same pretreatment processes.

Downloaded 04 Jul 2010 to 147.46.246.152. Redistribution subject to ECS license or copyright; see http://www.ecsdl.org/terms_use.jsp

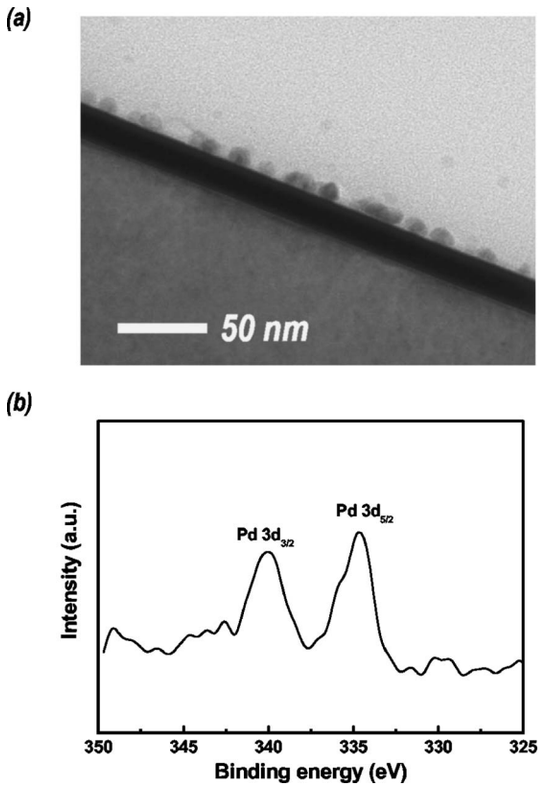

Figure 7. (a) Cross-sectional TEM image of Pd particles and (b) XPS 3d spectra of the Pd particles activated after Ta oxide etching and Sn sensitization.

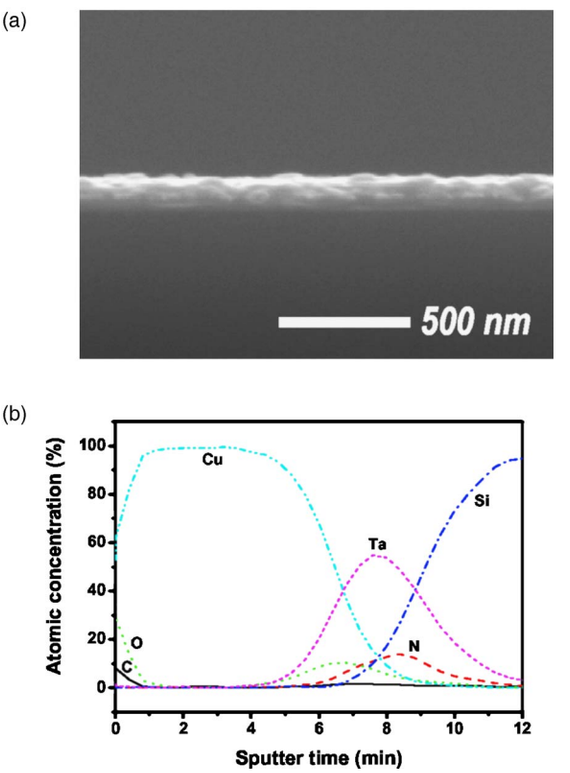

Figure 9. (Color online) (a) Cross-sectional SEM image of the Cu film deposited with the optimized conditions of Sn sensitization and Pd activation and (b) AES depth profile of the electroless Cu film.

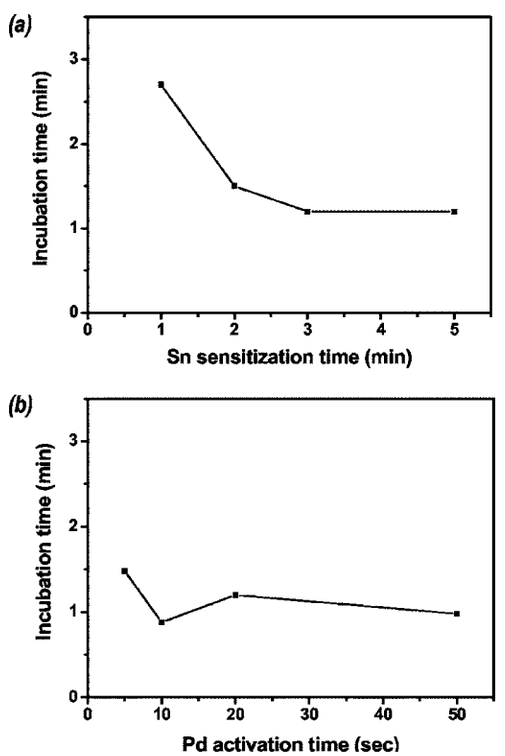

Figure 8. Changes in the incubation time as a function of (a) Sn sensitization time and (b) Pd activation time.

Conclusions

We performed Cu electroless deposition on a Ta substrate which had superior properties as a Cu diffusion barrier layer. As the CRM method and XPS analysis indicated, the addition of HNO_3 to a 1 vol % HF solution effectively removed the Ta oxide without increasing the surface roughness; it also assisted in the surface adsorption of Sn ions, which was an improvement from the 1 vol % HF solution alone. Sn sensitization created well-distributed and small sized Pd catalysts owing to improved wetting properties. The Sn sensitization and Pd activation time for Cu electroless deposition were optimized by measuring the incubation time and the resistivity of the film. Through the optimized conditions for Sn sensitization and Pd activation, a uniform Cu film could be deposited with a resistivity of 3.59 $\mu\Omega$ cm, which was decreased to 2.7 $\mu\Omega$ cm by a thermal annealing process.

Acknowledgments

This work was supported by KOSEF through the Research Center for Energy Conversion and Storage (RCECS), Dongbu Electronics, and by the Institute of Chemical Processes (ICP).

Seoul National University assisted in meeting the publication costs of this article.

References

1. Y. Shacham-Diamand and Y. Sverdlov, *Microelectron. Eng.*, **50**, 525 (2000).
2. S. Guan and B. J. Nelson, *Sens. Actuators, A*, **118**, 307 (2005).
3. J. E. Gray, P. R. Norton, R. Alnouno, C. L. Marola, M. A. Valvano, and K. Griffiths, *Biomaterials*, **24**, 2759 (2003).
4. M. E. Gertner and M. Schlesingers, *Electrochem. Solid-State Lett.*, **6**, J4 (2003).
5. C. Fukuhara, H. Ohkura, Y. Kamata, Y. Murakami, and A. Igarashi, *Appl. Catal., A*, **273**, 125 (2004).
6. H. Sun, G. Sun, S. Wang, J. Liu, X. Zhao, G. Wang, H. Xu, S. Hou, and Q. Xin, *J. Membr. Sci.*, **259**, 27 (2005).
7. C. H. Lee, S. C. Lee, and J. J. Kim, *Electrochem. Solid-State Lett.*, **8**, C110 (2005).
8. C. H. Lee, S. K. Cho, and J. J. Kim, *Electrochem. Solid-State Lett.*, **8**, J27 (2005).

Downloaded 04 Jul 2010 to 147.46.246.152. Redistribution subject to ECS license or copyright; see http://www.ecsdl.org/terms_use.jsp

9. A. Bauer, J. Ganz, K. Hesse, and K. Köhler, *Appl. Surf. Sci.*, **46**, 113 (1990).
10. H. M. Cheng, B. L. Zhou, Z. G. Zheng, Z. M. Wang, and C. X. Shi, *Plat. Surf. Finish.*, **77**, 130 (1990).
11. J. J. Kim and S. H. Cha, *Jpn. J. Appl. Phys., Part 1*, **41**, L1269 (2002).
12. M. Charbonnier, M. Alami, and M. Romand, *J. Electrochem. Soc.*, **143**, 472 (1996).
13. J. J. Kim and S. H. Cha, *Jpn. J. Appl. Phys., Part 1*, **40**, 7151 (2001).
14. S.-Y. Chang, C.-J. Hsu, R.-H. Fang, and S.-J. Lin, *J. Electrochem. Soc.*, **150**, C603 (2003).
15. W.-T. Tseng, C.-H. Lo, and S.-C. Lee, *J. Electrochem. Soc.*, **148**, C327 (2001).
16. H.-H. Hsu, C.-W. Teng, S.-J. Lin, and J.-W. Yeh, *J. Electrochem. Soc.*, **149**, C143 (2002).
17. A. E. Kaloyeros and E. Eisenbraun, *Annu. Rev. Mater. Sci.*, **30**, 363 (2000).
18. *Binary Phase Diagram*, T. B. Massalski, Editor, ASM International, Materials Park, OH (1990).
19. M. Takeyama, A. Noya, and A. Ohta, *J. Vac. Sci. Technol. B*, **14**, 3263 (1996).
20. B. Luanm, M. Yeung, W. Wells, and X. Liu, *Appl. Surf. Sci.*, **156**, 26 (2000).
21. W. E. Campbell and U. B. Thomas, *Trans. Electrochem. Soc.*, **76**, 303 (1939).
22. J. J. Kim and S.-K. Kim, *Appl. Surf. Sci.*, **183**, 311 (2001).
23. Q.-Y. Tong, Q. Gan, G. Fountain, P. Enquist, R. Scholz, and U. Gösele, *Appl. Phys. Lett.*, **85**, 3731 (2004).
24. S. Sapra, H. Li, Z. Wang, and I. I. Suni, *J. Electrochem. Soc.*, **152**, B193 (2005).
25. S. Siau, A. Vervaet, E. Schacht, and A. V. Calster, *J. Electrochem. Soc.*, **151**, C133 (2004).
26. C. H. Lee, S. Hwang, S.-C. Kim, and J. J. Kim, *Electrochem. Solid-State Lett.*, **9**, C157 (2006).

Downloaded 04 Jul 2010 to 147.46.246.152. Redistribution subject to ECS license or copyright; see http://www.ecsdl.org/terms_use.jsp